

Inelastic scattering effects and the Hall resistance in a 4-probe ring

G. Metalidis* and P. Bruno†

Max-Planck-Institut für Mikrostrukturphysik, Weinberg 2, D-06120 Halle, Germany‡

(Dated: February 8, 2020)

Phase randomizing processes in mesoscopic systems can be described in a phenomenological way within the Landauer-Büttiker formalism by attaching extra voltage probes to the sample. In this paper, it is shown that a perturbation treatment of this idea allows for the incorporation of such effects without the need of giving up the efficiency of recursive techniques commonly used for calculating the transmission coefficients. The technique is applied to a 4-probe ring, where a Hall effect can be observed that originates from quantum interference rather than a Lorentz force acting on the electrons. The influence of inelastic scattering on both the Hall resistance and the Aharonov-Bohm oscillations in the longitudinal resistance are examined.

I. INTRODUCTION

Quantum coherence plays a prominent role in the transport properties of mesoscopic systems; interference between different electron trajectories can lead to interesting effects like weak localization¹ and Aharonov-Bohm (AB) oscillations. Inelastic scattering events will destroy phase coherence and as such interference effects will be smeared out. Modelling inelastic scattering proves to be difficult because it is in general a many-body problem. However, a proposal has been put forward some years ago for incorporating these effects phenomenologically within the Landauer-Büttiker (LB) formalism (which is a single particle theory), by attaching extra voltage probes to the sample². Nevertheless, only few papers^{3,4} have made use of it because the widely used standard recursive Green's function method is unable to calculate the transmission coefficients between the extra voltage probes. As such, one should in principle invert the complete Hamiltonian to solve for all transmission coefficients which is of course computationally very inefficient for large systems. In this paper it will be shown how to treat the regime of weak inelastic scattering with a perturbation approach to the original voltage probe model, still keeping the computational effort the same as needed for the standard recursive Green's function method.

Our method is applied to a ring setup with 4 probes and a flux piercing through like depicted in Fig. 1. In such a setup a Hall voltage can be observed which is completely due to interference of electrons travelling in opposite directions along the ring, and which in principle does not rely on a Lorentz force acting on the electrons^{5,6}. In the current paper, numerical results for a realistic two-dimensional (2D) ring will be shown, taking into account inelastic scattering. The observed Hall effect disappears when decreasing the phase coherence length, showing again that the effect is solely due to quantum interference.

II. MODELING INELASTIC EFFECTS

For calculating resistances in our system, we will use the LB formalism which relates resistances to transmission probabilities between the leads. In the formalism, the leads are thought to be connected to large reservoirs with a well-defined chemical potential and temperature. The currents through the leads and the voltages on the reservoirs are related through (at temperature $T = 0$):

$$I_p = \frac{2e^2}{h} \sum_q T_{pq} (V_p - V_q), \quad (1)$$

where p, q label the leads/reservoirs and T_{pq} is the transmission probability from lead q to lead p . Although this formalism is only valid when phase coherence is present in the sample and the leads, phase breaking events must be taking place in the reservoirs in order for them to have a well-defined equilibrium distribution with a certain chemical potential. It is this insight that was used by Büttiker to arrive at the idea that an extra lead connected to a reservoir can introduce a phase breaking event². Indeed, if the current through such a lead is fixed to be zero (this is what we call a voltage probe), then for every electron that enters the lead and is absorbed by the reservoir, another one has to come out. But since equilibration is taking place in the reservoir, the electron coming out is not coherent with the one going in. In this way, it is possible to model inelastic effects in a phenomenological way.

In our calculations, we will attach a one-dimensional (1D) lead on every site of our tight binding model in order to have a homogeneous distribution of inelastic scattering centers. These leads can be thought to extend in a direction perpendicular to the 2D sample (see Fig. 1). An adequate choice of the potential in the 1D leads makes it possible that the influence of these leads can be described by just adding a complex onsite energy $-i\eta$ to every site in the lattice³. The parameter η is controlled by the hopping parameter between the 1D leads and the sample, and is related to the inelastic scattering time as $\eta = \hbar/2\tau_\varphi$. However, the approach goes further than just adding an imaginary potential; in order to conserve the total current in the system, one has to solve Eq. (1)

so that the current through the extra 1D leads is zero. Before giving expressions for the currents through the leads, we will introduce some notation: the 1D voltage probes attached to the system to simulate phase randomizing processes are labelled by a Greek index, while the real physical leads connected to the sample (referred to as contacts from now on) will be labelled by letters m, n, \dots . Now, by putting $I_\alpha = 0$ for all α , and solving for the voltages V_α on the voltage probes in terms of the voltage differences $V_n - V_m$ between the contacts, one can obtain an expression for the currents I_n through the contacts similar to Eq. (1), but now with effective transmission probabilities incorporating the effect of the voltage probes:

$$I_n = \frac{2e^2}{h} \sum_m T_{nm}^{\text{eff}} (V_n - V_m), \quad (2)$$

where the effective transmission probabilities can be written as follows:

$$T_{nm}^{\text{eff}} = T_{nm} + \sum_\alpha \frac{T_{n\alpha} T_{\alpha m}}{S_\alpha} + \sum_\alpha \sum_{\beta \neq \alpha} \frac{T_{n\alpha} T_{\alpha\beta} T_{\beta m}}{S_\alpha S_\beta} + \dots, \quad (3)$$

with $S_\gamma = \sum_l T_{\gamma l} + \sum_{\delta \neq \gamma} T_{\gamma\delta}$. This expression has a clear physical interpretation: the first term describes transmission from contact m to contact n without any inelastic process, the next term incorporates a single scattering event, then double scattering and so on.

A standard method commonly employed (because of its efficiency) for calculating the transmission coefficients is the recursive Green's function technique (reviewed in Ref. 7). However, this technique can give only access to the transmission coefficients between the contacts T_{nm} . For calculating the effective transmission coefficients in Eq. (3), one would also need the transmission probabilities between the contacts and the voltage probes ($T_{n\alpha}$ and $T_{\alpha m}$), and between the voltage probes themselves ($T_{\alpha\beta}$). These are unavailable with the standard technique, because one would need Green's functions connecting points at the edges of the sample (where the contacts are attached) with points inside the sample, whereas the technique only gives us Green's functions between the left and right edge.

However, one could neglect all terms in Eq. (3) involving two and more scattering events (by putting $T_{\alpha\beta} = 0$), and keep only the direct transmission term together with the single scattering term. This approximation is valid when the phase coherence length of the sample is larger than the system size. Although the standard technique still cannot give access to $T_{n\alpha}$ needed for the second order term, a recursive technique has been developed recently that allows to calculate these with the same numerical effort needed for the standard recursive Green's function method. Details of this technique can be found in Ref. 8. In that way we are able to treat the effective transmission coefficients to second order in the phase randomization processes.

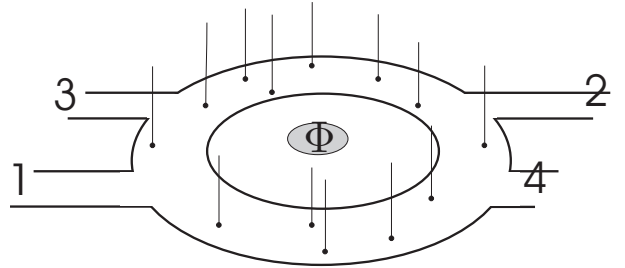


FIG. 1: Schematic view of the 4-probe ring setup. Inelastic scatterers will be modelled by attaching a 1D lead at every scattering center. In real calculations, every site of the tight binding model is attached to a voltage probe in order to have homogeneous scattering.

It should be noted that by neglecting higher order terms in Eq. (3), one will break current conservation rules whenever a magnetic flux is present in the system; but in the weak scattering regime, this error will be small. In all calculations we present, the sum of currents flowing through leads 1 to 4 divided by the sum of their absolute values was smaller than 10^{-4} .

III. RESULTS FOR A 4-PROBE RING

We will consider a 4-probe ring in a two-dimensional electron gas, like shown schematically on Fig. 1. All leads are arranged to the left and right of the ring for computational convenience. The Hamiltonian of the system can be written as:

$$H = \frac{1}{2m^*} (\mathbf{p} - e\mathbf{A})^2 + V_{\text{imp}} + V_c, \quad (4)$$

where m^* and e are respectively the effective mass and charge of the electron, \mathbf{A} is the vector potential created by the flux through the ring, V_c is the confinement potential defining the ring, and V_{imp} is the elastic impurity potential. By discretizing this Hamiltonian on a square lattice with lattice parameter a , one obtains a tight binding model:

$$H = \sum_n \sum_m \epsilon_{mn} |m, n\rangle \langle m, n| + (t_{m,n}^x |m, n+1\rangle \langle m, n| + t_{m,n}^y |m+1, n\rangle \langle m, n| + h.c.),$$

with (m, n) labelling the sites on the lattice, and ϵ_{mn} the on-site energies. The hopping parameters are given by:

$$t_{mn}^{x(y)} = -t e^{-i e / \hbar \int \mathbf{A} \cdot d\mathbf{l}}, \quad (5)$$

with the integral evaluated along the hopping path and $t = \hbar^2 / 2m^* a^2$.

The ring parameters were chosen in accordance to typical rings fabricated experimentally in a 2DEG at the interface of an GaAs-AlGaAs heterostructure. The density of the 2DEG was chosen to be $n_s = 4 \times 10^{11} \text{ cm}^{-2}$,

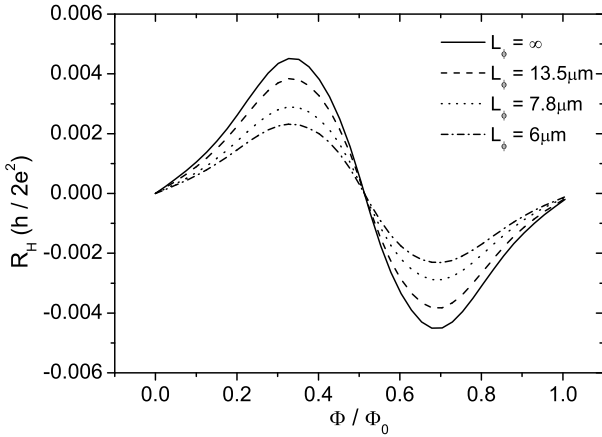


FIG. 2: The Hall resistance $R_H = 1/2(R_{12,34} - R_{34,12})$ for different values of the phase coherence length.

corresponding to a Fermi wavelength of 40 nm. The ring has a mean radius of $0.6 \mu\text{m}$, and the width of the arms is 200 nm, so that 10 channels are available for conduction. The mobility of the electron gas is $\mu = 5 \times 10^5 \text{ cm}^2 \text{ V}^{-1} \text{ s}^{-1}$, giving a mean free path of $5.2 \mu\text{m}$.

This translates into the following tight binding parameters. The lattice parameter was chosen to be $a = 6.7 \text{ nm}$, so that $\lambda_F = 6a$ and the Fermi energy $E_F = 1.1t$. The mean radius of the ring is $89a$, and the width $29a$. Elastic scattering was modelled with on-site energies distributed randomly in the interval $[-0.127t, 0.127t]$, which gives a mean free path of $l_m = 780a$ (estimated in Born approximation).

For this ring, we will calculate both the longitudinal resistance $R_{12,12}$ and the transverse resistances $R_{12,34}$ and $R_{34,12}$ (see Fig. 1), and the influence of inelastic processes on the results will be made clear. We use the common notation $R_{kl,mn} = (V_m - V_n)/I_k$ for a measurement where current is supplied through contacts k and l , and the voltage difference $V_m - V_n$ is measured, fixing $I_m = I_n = 0$. In terms of transmission coefficients, these resistances are given by⁹:

$$R_{kl,mn} = \frac{T_{mk}T_{nl} - T_{nk}T_{ml}}{D}, \quad (6)$$

where D is a 3×3 subdeterminant of the matrix A relating the currents through the four contacts to their voltages [$I_m = A_{mn}V_n$, c.f. Eq. (1)]⁹. D is independent of the indices $klmn$. When inelastic processes are included, the transmission coefficients in these expressions have to be replaced with the effective probabilities given in Eq. (3).

Let's look at the resistance $R_{12,34}$. Suppose an electron enters the ring through lead 1. It can reach lead 3 by different paths: there is a direct path between lead 1 and lead 3, but there is also a trajectory going like $1 \rightarrow 4 \rightarrow 2 \rightarrow 3$. These two trajectories will interfere with each other, and fix the voltage on lead 3 (neglecting paths circling the ring more than once). The same can be

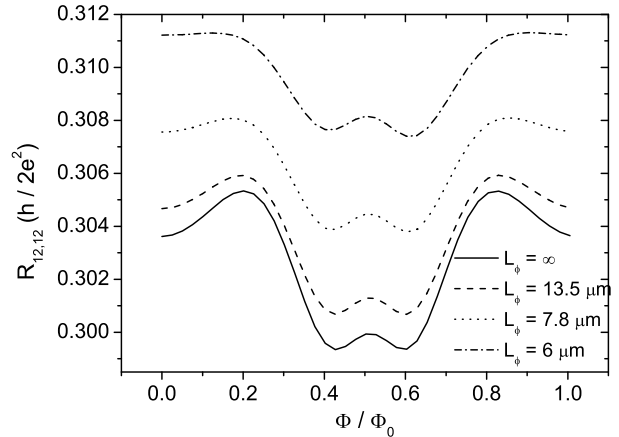


FIG. 3: Longitudinal resistance of a 4-probe ring for different values of the phase coherence length.

applied to lead 4: again there is a direct and indirect path interfering and setting the voltage on lead 4. It is clear that because of symmetry, the voltage on lead 3 and lead 4 will be the same when no flux is present through the ring. However, when a flux pierces through the ring, time reversal symmetry is broken and the phase difference between both paths going from 1 to 3 is different from that for the paths going from 1 to 4, so that a voltage difference $V_3 - V_4$ will develop. For a one-dimensional ring, this effect is described in some detail in Ref. 5, and numerical calculations for a simple model are shown in Ref. 6. The effect is purely based on interference; a Hall voltage will also be present when the magnetic field is limited to the inside of the ring, and no flux is going through the arms of the ring. Like in the original Aharonov-Bohm proposal, the electron can feel the vector potential, and is not subjected to a real Lorentz force.

The Hall resistivity is the anti-symmetric part of the resistivity tensor: $\rho_H = 1/2(\rho_{xy} - \rho_{yx})$. In our case this comes down to calculating the Hall resistance $R_H = 1/2(R_{12,34} - R_{34,12})$, which is the transverse resistance part that is anti-symmetric with respect to the magnetic flux⁹. Results are shown in Fig. 2. The Hall resistance varies periodically with the magnetic flux through the ring, the period being the fundamental flux quantum Φ_0 . In the figures, only one fundamental period is shown. It should be mentioned again that there is no flux through the ring arms, so the flux is fully contained within the ring. The interesting effect is that for nonzero flux, a Hall resistance can be measured, which is not due to a Lorentz force, but which originates from interference between different trajectories along the ring like explained previously.

Phase randomizing processes are included in the way explained in the previous section. The phase coherence length of the sample is given by $L_\varphi = \sqrt{D\tau_\varphi}$, where $D = 1/2v_F l_m$ is the diffusion constant, and $\tau_\varphi = \hbar/2\eta$ is the phase relaxation time. The parameter η corresponds to the hopping parameter between the attached voltage

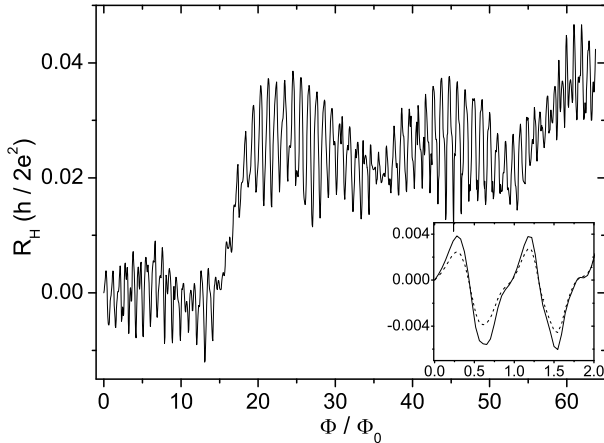


FIG. 4: Hall resistance R_H of the 4-probe ring when a magnetic field is applied across the whole sample. Φ is defined as the flux through the mean radius of the ring. The effect of inelastic scattering is shown in the inset, for the first 2 oscillations in the resistance: $L_\varphi = \infty$ (solid line) and $L_\varphi = 7.8\mu\text{m}$ (dashed).

probes and the sample. For our system, we varied the phase coherence length between $6\mu\text{m}$ and infinity, which is clearly in the range of validity of our approximation (system size $> L_\varphi$). When the phase coherence length is reduced (dashed and dotted lines in the Fig. 2), one can see that the amplitude of the oscillations decreases. This was to be expected because the Hall effect we observe is completely due to quantum interference.

Turning to Fig. 3, the normal AB oscillations are observed in the longitudinal resistance. Furthermore, one sees that the influence of inelastic scattering on the longitudinal resistance is twofold. Firstly, the mean value of the resistance will increase by decreasing the phase coherence length because we are introducing extra scatterers. Second, the amplitude of the AB oscillations decreases with decreasing coherence length, because these oscillations are the result of interference effects.

When comparing the magnitude of the Hall resistance in Fig. 2 with the longitudinal resistance shown in Fig. 3, we see that the oscillations have the same order of magnitude. Since normal Aharonov-Bohm (AB) oscillations

can be observed experimentally quite easily nowadays, this means that it is also feasible to measure the Hall effect in the 4-probe ring.

However, in an experimental setup it is difficult to confine the magnetic flux to a region inside the ring, and therefore the magnetic field is applied across the whole sample. In Fig. 4, we show calculation results for this case. The Hall resistance R_H is not anymore strictly periodic with respect to the flux. Nevertheless quasi-periodic oscillations are visible resulting from quantum interference, whose amplitude will decrease when introducing inelastic scattering (see the inset of Fig. 4). A beating pattern can be observed in the oscillations, which is a result of having several channels open for conduction in the ring arms; trajectories for different channels surround slightly different areas and thus fluxes. Compared to Fig. 2, the Hall resistance also gets a non-zero offset: this contribution is a result of the Lorentz force acting on the electrons when there is a flux present in the ring arms.

IV. CONCLUSION

Incorporating the effect of phase randomizing processes in a phenomenological way can be done with the attachment of extra voltage probes to sample, an idea originally proposed by Büttiker². In this paper, we have described a method for treating inelastic effects based on this idea, but such that a recursive technique for calculating the transmission coefficients can still be used. Doing so, one is able to treat the problem in a numerically very efficient way, which was not possible within the original proposal. The approach however consists of neglecting multiple inelastic scattering and is therefore only valid in a regime where the phase coherence length is larger than the system size.

The method was applied to an experimentally realizable ring with four attached contacts, and a Hall effect was observed which is due to quantum interference rather than an implicit Lorentz force acting on the electrons. This Hall effect disappears with decreasing the phase coherence length.

* Electronic address: georgo@mpi-halle.de

† Electronic address: bruno@mpi-halle.de

‡ URL: <http://www.mpi-halle.de>

¹ G. Bergmann, Phys. Rep. **107**, 1 (1984).

² M. Büttiker, Phys. Rev. B **32**, 1846 (1985).

³ J. L. D'Amato and H. M. Pastawski, Phys. Rev. B **41**, 7411 (1990).

⁴ F. Gagel and K. Maschke, Phys. Rev. B **54**, 13885 (1996).

T. Ando, Surf. Science **361/362**, 270 (1996).

⁵ S. J. Robinson, J. Phys.: Condens. Matter **7**, 6675 (1995).

⁶ P. Gartner and A. Aldea, Z. Phys. B **99**, 367 (1996).

⁷ D. K. Ferry and S. M. Goodnick, *Transport in Nanostructures*, (Cambridge University Press, England, 1997).

⁸ G. Metalidis and P. Bruno, Phys. Rev. B **72**, 235304 (2005).

⁹ M. Büttiker, Phys. Rev. Lett. **57**, 1761 (1986).